Temperature dependence of Raman scattering in $Ge_{1-x}Si_x$ alloys

Hubert H. Burke and Irving P. Herman

Department of Applied Physics, Columbia University, New York, New York 10027

(Received 18 March 1993)

First-order Raman scattering of polycrystalline $Ge_{1-x}Si_x$ alloys is studied from $T = 300-900$ K. The Raman shifts of the three optical phonons are modeled by considering thermal expansion and coupling to two phonons. The shift of the Si-Si mode near 500 cm^{-1} has a temperature dependence similar to that of c-Si for $x > 0.7$, but has a slower temperature variation for more Ge-rich alloys. The Ge-Ge mode near 300 cm^{-1} has a temperature dependence similar to that of the optical-phonon mode in c-Ge for all compositions studied. The Raman shift of the Ge-Si mode has a dependence in between that of the Ge-Ge and Si-Si modes. Also, the Raman linewidths of the Si-Si and Ge-Ge modes have a temperature dependence similar to that of c-Si and c-Ge, respectively.

I. INTRODUCTION

Recent interest in $Ge_{1-x}Si_x$ alloys is motivated by their fundamental properties and technological importance. The properties of these compositionally disordered alloys are similar to those of Si and Ge in some ways, while in other ways they are quite different.[1,2] Of particular interest here, the first-order Raman spectrum of GeSi alloys has three peaks; two are similar to the optical phonon peaks in pure Si and Ge, while the third, due to nearest-neighbor Ge-Si pairs, is very different. The dependence of first-order Raman scattering of optical phonons in Si and Ge on temperature has been examined in several theoretical and experimental investigations.[3-15] This has led to a better understanding of the anharmonicity in diamond structure crystals, and has provided data needed for diagnostic applications, such as *in situ* measurements of temperature.[15,16] Previous studies of Raman scattering in GeSi alloys have concentrated on phonon properties at ambient and lower temperatures.[17-21] In this paper we present an investigation of first-order Raman scattering in bulk polycrystalline GeSi alloys as a function of temperature.

Raman spectra of $Ge_{1-x}Si_x$ alloys are characterized by three main peaks near 300, 400, and 500 cm^{-1}, which are attributed to optic modes of Ge-Ge, Ge-Si, and Si-Si atom pairs, respectively.[18-21] Additional weak structure between 420 and 470 cm^{-1} has also been observed. On the basis of a lattice-dynamical calculation, Alonso and Winer[17] associated these minor peaks with localized Si-Si motion in the vicinity of several Ge atoms. The shifts and linewidths of the three main Raman peaks have been measured at room temperature by Renucci, Renucci, and Cardona[18] and Brya[19] over the entire composition range. The composition dependence of the peak positions calculated with an isodisplacement model agree well with experiment.[22]

The addition of Si (Ge) to an initially pure Ge (Si) crystal softens the Ge-Ge (Si-Si) mode, with the Si-Si mode frequency exhibiting a greater dependence on concentration than the Ge-Ge mode frequency. The Ge-Ge mode has a weaker composition dependence because the competing effects of local strain and confinement partially cancel for this mode, whereas they add for the Si-like mode. Recent experiments have shown that the frequency of the Ge-Ge mode initially increases slightly for very low concentrations of Si.[21] The Ge-Si mode is associated with the optical modes of an ordered zinc-blende GeSi lattice. The frequency of this mode increases rapidly as Si is added to Ge, attains a maximum near $x = 0.5$, and decreases more slowly for $x > 0.5$.

The Raman spectra of c-Si and c-Ge change with temperature due to the anharmonicity of the vibrational potential energy. Several studies have described how the Raman shift decreases as the temperature increases. Hart, Aggarwal, and Lax[6] measured the peak position for Si over the temperature range 20-770 K, while Balkanski, Wallis, and Haro[4] reported the frequency shifts for Si from 5 to 1400 K. Menendez and Cardona[3] measured the temperature dependence of the first-order Raman scattering by phonons in both Si and Ge. Raman measurements of the solid semiconductor at the melting temperature have been made by Nemanich *et al.*[12] on Si, and by Tang and Herman[13] on Si and Ge.

The molecular-dynamics calculation by Wang, Chan, and Ho[11] has been used to predict the Raman spectrum of optical-phonon scattering in silicon. Their results are in excellent agreement with the Raman data for $T = 300-1000$ K. Most other theoretical work on optical phonons in Si and Ge to date has been based on perturbation theory. In this approach, the change in the phonon frequency, the real part of the phonon self-energy, is caused by changes of volume with T and by phonon-phonon coupling. Early theoretical calculations by Cowley,[8] based on a shell model with empirically determined force constants, included the cubic term to second order and fit the frequency shift fairly well. Simplifying Cowley's approach, Klemens[9] modeled the optical-phonon decay as a single-channel process involving decay into (only) identical acoustical-phonon pairs (three-phonon process). Balkanski, Wallis, and Haro[4] found it necessary to extend the Klemens model to include coupling to three identical phonons (four-phonon process) to fit their high-temperature data for c-Si. Menendez and

Cardona[3] included the thermal-expansion contribution in their analysis of the frequency shift and claimed, on the basis of density-of-states considerations, that optical-phonon coupling to LA-LO-phonon pairs is the most significant coupling mechanism at moderate temperatures. Narasimhan and Vanderbilt[14] used their first-principles determination of anharmonic force constants in Si to analyze the importance of cubic anharmonicity terms in Raman scattering. By using conservation of energy and momentum they found coupling only to pairs of LA-TA phonons, and not to pairs of LA-LO phonons as suggested by Menendez and Cardona. Tang and Herman[13] used their data and results from earlier studies to compare the various existing models. They showed that the Raman shift is successfully modeled by including thermal expansion and coupling to two phonons.

No Raman measurements at elevated temperatures have been published for the GeSi alloy system. Such measurements can further the understanding of phonon processes in these disordered solids, where there is positional order (at the lattice sites) and chemical disorder (describing which atom is at a given site). This can be fundamentally different from phonon coupling in perfect crystals, where there is both positional and chemical order, and in amorphous solids, where there is positional disorder. The dependence of the real part of the phonon self-energy on T may also differ in GeSi alloys vis à vis c-Si and c-Ge because the mode Grüneisen parameters for the alloy are different.[23−27]

Renucci, Renucci, and Cardona[18] measured the Raman spectrum of bulk polycrystalline Ge-Si alloys over the entire composition range at 77 and 295 K. For this low-temperature regime, their results suggest that the change in the mode frequencies with temperature is the same for each mode and is independent of concentration. Herman and Magnotta[16] used local laser heating of GeSi alloys to follow the decrease of the mode frequencies with increasing laser power (and therefore temperature). Because the laser heating produced a nonuniform temperature distribution, they could not explicitly analyze the temperature dependence.

II. EXPERIMENTAL PROCEDURE AND RESULTS

Polycrystalline $Ge_{1-x}Si_x$ alloys, with an average grain size of 10–20 μm as determined by scanning electron microscopy, were grown by the horizontal Bridgeman technique.[28] Slow growth rates ($\sim 10^{-5}$ cm/s) were employed in order to make good quality, homogeneous material.[29] The composition of the alloy ingots changed monotonically along the growth direction due to normal directional freezing of the melt. The ingots were cut perpendicular to the growth axis to obtain samples.

The compositions of three samples ($x = 0.15$, 0.59, and 0.92) were determined by Auger-electron spectroscopy (AES). These results agreed with the room-temperature Raman measurements of Renucci, Renucci, and Cardona.[18] The compositions of the other samples ($x = 0.20$, 0.29, 0.57, 0.60, 0.70, and 0.91) were determined only by Raman scattering.[18,30] Raman microprobe scattering in-

dicated that the samples were quite homogeneous. Within a 25-μm radius the line shift of the Si-Si mode varied by ± 1.0 cm^{-1}, compared to the ± 0.5-cm^{-1} measurement uncertainty. In general, the linewidths of the GeSi alloys examined here are greater than those reported in Refs. 18 and 19 by $\sim 2-5$ cm^{-1}, even after annealing.

Stokes Raman measurements were made in the backscattering configuration using a cw argon-ion laser (4880 Å) for all of the samples. c-Ge spectra were also acquired with a cw krypton-ion laser (6471 Å). The laser power was <40 mW and the laser spot size was 25 μm (or larger), so the estimated temperature rise due to laser heating was <20 K.

The Raman signal was analyzed with a triple spectrometer, detected with an intensified diode array, and calibrated with atomic line sources. The high- and low-energy sides of these asymmetric Raman peaks were fit with separate Lorentzians, with full widths at half maximum Γ_H and Γ_L, respectively ($\Gamma_H < \Gamma_L$). The peak widths were obtained after correcting for instrumental broadening, which was fit by a Lorentzian with an ~ 2.8-cm^{-1} full width at half maximum (FWHM).

The Raman spectra of c-Si, c-Ge, and five $Ge_{1-x}Si_x$ alloys ($x = 0.15$, 0.29, 0.59, 0.70, and 0.92) were acquired from $300 - \sim 880$ K. Representative alloy Raman spectra are shown in Fig. 1. The sample chamber, which was housed in the furnace, was filled with Ar (835 Torr) to prevent oxidation. Measurements were made both during ramp-up heating and during cooling; within experimental uncertainty the spectra were the same. The Raman spectra obtained at room temperature after cooling were essentially the same as the initial room-temperature spectra. Four alloys ($x = 0.20$, 0.57, 0.60, and 0.91) were examined at ~ 77 and 300 K, and showed the same low-temperature dependence as seen in Ref. 18.

As the temperature increases, the Raman shift (ω) decreases, the peak intensity decreases, and the Raman linewidth (Γ) increases, as is shown in Fig. 1 for the
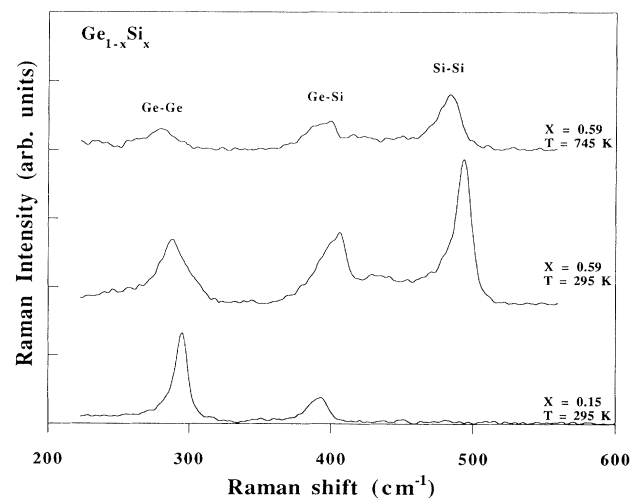

FIG. 1. Typical Raman spectra of $Ge_{1-x}Si_x$ alloys, with the three modes denoted.

$x = 0.59$ alloy. The dependence of the Raman line shift on temperature in c-Si and c-Ge is compared with results from previous studies in Figs. 2(a) and 2(b), respectively. The Raman shifts and linewidths for c-Si, c-Ge, and the alloys measured here are plotted in Figs. 3 and 4. The plotted linewidths (FWHM) are $\Gamma = (\Gamma_H + \Gamma_L)/2$. Γ_H and Γ_L have the same dependence on temperature, i.e., $\Gamma_H(T)$ and $\Gamma_L(T)$ differ by a constant. The linewidth data have significantly more scatter than those for the line shifts, and the linewidths could not be adequately determined for several modes.

The Raman shifts in c-Ge were consistently ~ 1 cm^{-1} smaller than those measured in Ref. 3; there is no such trend for c-Si (Fig. 2). Within experimental uncertainty, the Raman shifts obtained for c-Ge were the same with either 4880 or 6471 Å. Reference 31 reported slightly smaller $\omega_{c\text{-Ge}}(T)$ using 5145 Å than with 6328 Å, which was attributed to the larger contribution of lower ω surface phonons with 5145 Å. Menendez and Cardona[3] made their measurements on c-Ge with 6471 Å. The data in Fig. 2 were fit with a straight line. For c-Si, $d\omega/dT = -0.0247$ cm^{-1}/K here, compared to -0.022 and -0.031 cm^{-1}/K in Refs. 3 and 4, respectively. For c-Ge, $d\omega/dT = -0.0200$ cm^{-1}/K here, compared to -0.018 and -0.025 cm^{-1}/K in Refs. 3 and 7, respec-

FIG. 3. Raman shifts of the three Ge$_{1-x}$Si$_x$ alloy modes as a function of temperature, for different alloy concentrations. The experimental uncertainty in the shift is ± 0.25 cm^{-1} for $T < 600$ K, and ± 0.50 cm^{-1} for $T > 600$ K. The solid lines are fits using Eqs. (1)–(4) with parameters given in Table II for each mode and composition.

tively. Agreement with earlier work is good, particularly with Ref. 3.

$\omega(T = 0)$ and $d\omega/dT$ obtained from least-squares linear fits to the Raman shifts in Fig. 3 are given in Table I. Adding Ge to a Si-rich alloy does not change

TABLE I. Linear fit of the Raman shift vs temperature in the range 295–900 K for Ge$_{1-x}$Si$_x$ alloys. The error in $d\omega/dT$ is ± 0.0008 cm^{-1}/K.

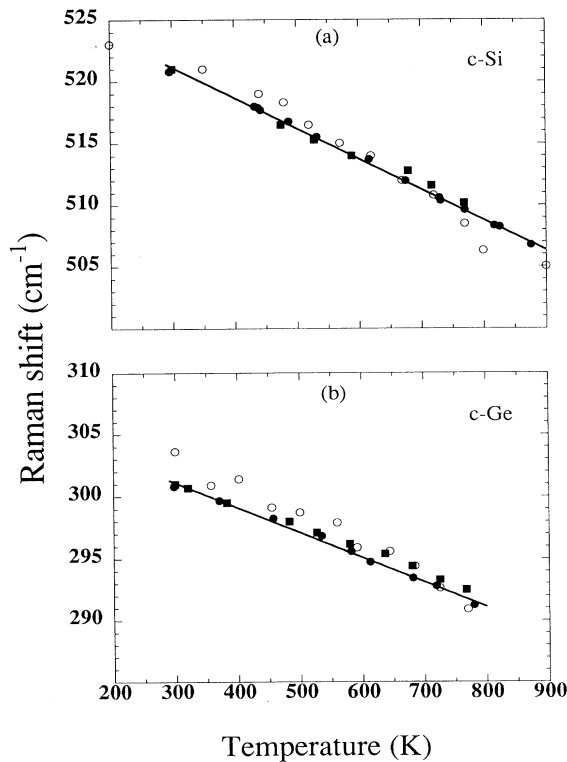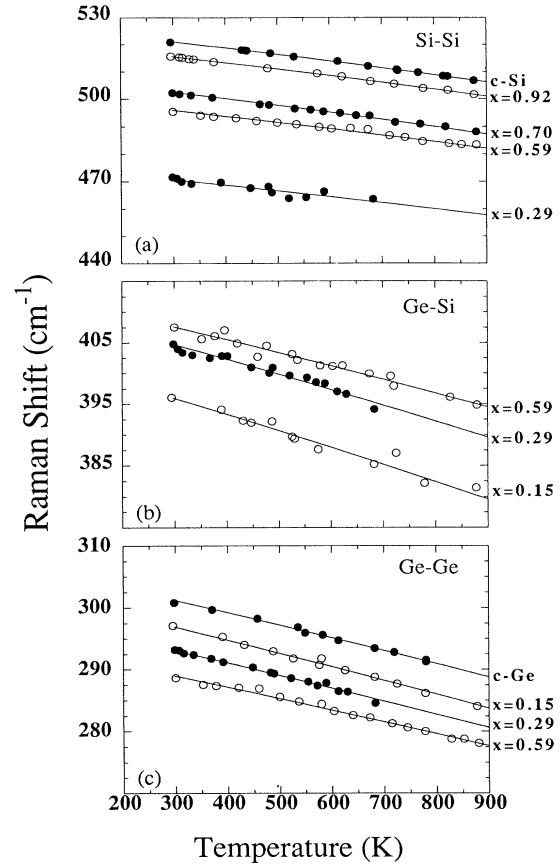| Mode	x	$\omega(T=0)$ (cm^{-1})	$d\omega/dT$ (cm^{-1}/K)
c-Si	1.0	528.6	−0.0247
Si-Si	0.92	522.7	−0.0239
	0.70	509.4	−0.0238
	0.59	501.8	−0.0211
	0.29	476.9	−0.0207
Ge-Si	0.59	414.1	−0.0215
	0.29	411.5	−0.0232
	0.15	403.7	−0.0259
Ge-Ge	0.59	294.7	−0.0187
	0.29	299.5	−0.0210
	0.15	303.9	−0.0225
c-Ge	0.0	307.1	−0.0200

FIG. 2. Raman shifts of (a) c-Si and (b) c-Ge as a function of temperature from several experiments. The squares are data from Ref. 3, the open circles in (a) and (b) are data from Refs. 4 and 7, respectively, and the solid circles are from this experiment, for which the uncertainty is ± 0.25 cm^{-1} for $T < 600$ K, and ± 0.50 cm^{-1} for $T > 600$ K.
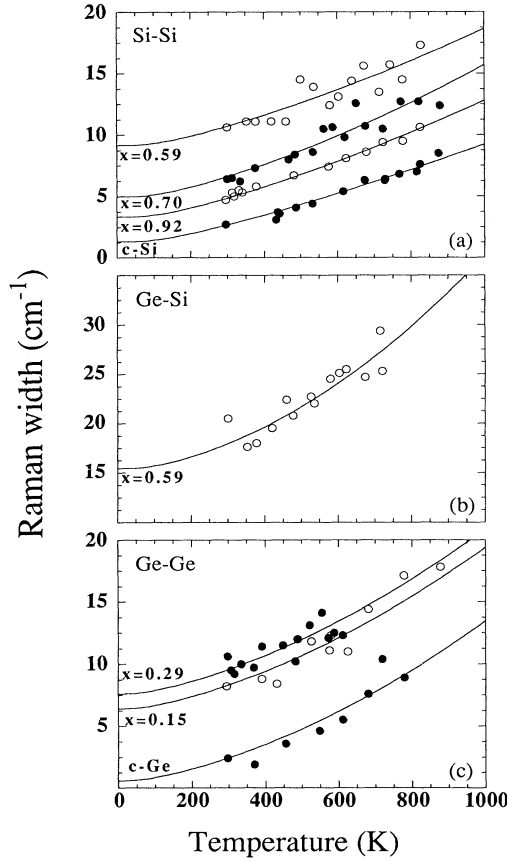
FIG. 4. Raman linewidths of the three $Ge_{1-x}Si_x$ alloy modes as a function of temperature, for different alloy concentrations. The experimental uncertainty in the width is $\sim \pm 4\%$. The solid lines are fit using Eq. (5), with parameters given in Table III for each mode and composition, with the exception of curve drawn through the $x = 0.29$ Ge-Ge data. For ease of viewing, this curve was plotted with the B_{1i} and B_{2i} of the $x = 0.15$ Ge-Ge mode. The data for c-Ge were corrected by using the 2.3-cm^{-1} instrumental linewidth for that run, and not the average value (2.8 cm^{-1}) used for the other runs.

c-Ge (Refs. 3 and 4) are extended here to describe each of the three alloy modes. The damped frequency of the Raman-active optical mode is[4]

$$\omega_i(T) = \omega_{0i} + \Delta_i(T) , \qquad (1)$$

where ω_{0i} is the harmonic frequency of the optical mode for the mode ($i =$ Si-Si, Ge-Si, and Ge-Ge) and $\Delta_i(T)$ is the perturbation of the real part of the phonon self-energy. $\Delta_i(T)$ can be expressed as

$$\Delta_i(T) = \Delta_i^{(1)}(T) + \Delta_i^{(2)}(T) \qquad (2)$$

where $\Delta_i^{(1)}(T)$ is due to thermal expansion and $\Delta_i^{(2)}(T)$ is due to phonon-phonon coupling.

The thermal-expansion contribution for mode i is[32]

$$\Delta_i^{(1)}(T) = \omega_{0i} \left[\exp\left\{ -3\gamma_i \int_0^T \alpha(T')dT' \right\} - 1 \right] , \qquad (3)$$

where $\alpha(T)$ is the coefficient of linear thermal expansion, and γ_i is the mode Grüneisen parameter.

$\Delta_i^{(1)}(T)$ depends on alloy composition because α, γ_i, and ω_{0i} are functions of x; further, γ_i and ω_{0i} are different for the three modes. With decreasing Si fraction, α_{GeSi} increases from α_{Si} (2.59×10^{-6}/K) to α_{Ge}(5.90×10^{-6}/K) at 300 K, first slowly from $x \sim 1$ to 0.15 and then much more rapidly for $x < 0.15$.[33] From 300–875 K, α_{Si} increases monotonically by $\sim 50\%$, α_{Ge} by $\sim 20\%$, and α_{GeSi} by an intermediate amount. ω_{0i}, as will be determined from fitting $\omega(T)$, and γ_i (Ref. 27) are listed in Table II. Note that γ_{Si-Si} increases with increasing Ge fraction, while γ_{Ge-Ge} increases with increasing Si fraction. For each mode, the decrease of ω_i with T due to thermal expansion becomes more rapid as the Ge fraction increases, because $\gamma_i(x)\alpha(x)$ always increases with the Ge fraction.

The anharmonic coupling term $\Delta^{(2)}(T)$ is due to cubic, quartic, and higher-order anharmonic terms in the Hamiltonian. Following the approach for c-Si and c-Ge,[4] it is approximated by

$d\omega_{Si-Si}/dT$ much until $x < 0.7$, and then the magnitude of the slope decreases with increasing Ge fraction. $|d\omega_{Ge-Ge}/dT|$ is higher for $x = 0.15$ (85% Ge) than for c-Ge, and it then decreases with increasing Si fraction. In general, for both the Si-Si and Ge-Si modes, a change in the alloy fraction that decreases ω also decreases $|d\omega/dT|$, though at a faster rate. In contrast, $|d\omega_{Ge-Si}/dT|$ increases with decreasing Si fraction (for $x = 0.59$–0.15), even though ω_{Ge-Si} decreases. Though $\omega_{Ge-Ge} < \omega_{Ge-Si} < \omega_{Si-Si}$, the slopes $d\omega/dT$ for the three modes are in general comparable. In particular, the magnitude of the fractional change with T $|(d\omega/dT)/\omega|$ is largest for the Ge-Ge mode, intermediate for the Ge-Si mode, and smallest for the Si-Si mode.

III. ANALYSIS OF THE RAMAN SPECTRA

The perturbation models that have successfully described Raman scattering of optical phonons in c-Si and

TABLE II. Parameters for fitting the Raman shift $\omega(T)$ for $Ge_{1-x}Si_x$ alloys with the $f_1 = 0.35, f_2 = 0.65$, $A_2 = 0$ model, using the data in Fig. 3. γ_i are obtained from Ref. 27. The uncertainty in A_{1i} is estimated to be ± 0.1 cm^{-1}.

Mode	x	γ_i	ω_{0i} (cm^{-1})	A_{1i} (cm^{-1})	$\omega(T=0)$ (cm^{-1})
c-Si	1.0	1.02	528.0	-3.4	524.6
Si-Si	0.92	1.09	522.2	-3.1	519.1
	0.70	1.19	509.4	-3.0	506.4
	0.59	1.25	501.8	-2.4	499.4
	0.29	1.42	476.0	-1.8	474.2
Ge-Si	0.59	1.19	413.3	-2.1	411.2
	0.29	1.20	411.6	-2.4	409.2
	0.15	1.26	403.4	-2.5	400.9
Ge-Ge	0.59	1.28	293.8	-1.3	292.5
	0.29	1.19	298.6	-1.5	297.1
	0.15	1.15	302.8	-1.6	301.2
c-Ge	0.0	1.11	306.4	-1.4	305.0

$$\Delta_i^{(2)}(T) = A_{1i}\left\{1 + \sum_{j=1}^{2} \frac{1}{(e^{x_j}-1)}\right\}$$
$$+ A_{2i}\left\{1 + \sum_{k=1}^{3}\left[\frac{1}{(e^{y_k}-1)} + \frac{1}{(e^{y_k}-1)^2}\right]\right\},$$

(4)

where $x_1 + x_2 = y_1 + y_2 + y_3 = \hbar\omega_{0i}/k_B T$. The first term couples the optical phonon to two phonons (three-phonon coupling), while the second term represents higher-order processes that couple it to three phonons (four-phonon coupling). As $T \to 0$, $\omega_i \to \omega_{0i} + A_{1i} + A_{2i}$. In the high-temperature limit ($k_B T \gg \hbar\omega_{0i}$), $\Delta_i^{(1)}(T)$ and the first term in $\Delta_i^{(2)}(T)$ vary linearly with T, while the second term in Eq. (4) varies as T^2. In this limit the slope of the three-phonon term in $\Delta_i^{(2)}(T)$ is $A_{1i}k_B/\hbar\omega_{0i}(1/f_1 + 1/f_2)$, where $x_j = f_j\hbar\omega_{0i}/k_B T$ and $f_1 + f_2 = 1$.

The Raman shift data are analyzed assuming that in three-phonon coupling either $f_1 = f_2 = 0.5$ or $f_1 = 0.35$, $f_2 = 0.65$. The fits include the thermal-expansion contribution $\Delta^{(1)}(T)$, and either exclude four-phonon coupling ($A_2 = 0$) or include it (assuming that $y_k = \hbar\omega_{0i}/3k_B T$).[4] They were obtained by using a least-squares fit of $\omega(T)$ to determine A_{1i}, with ω_{0i} chosen so that $\omega_{0i} + A_{1i}$ is close to $\omega_i(T = 77$ K). Menendez and Cardona[3] showed that the three-phonon model with $f_1 = 0.35$, $f_2 = 0.65$, which couples the optical phonon to phonons with energy $0.35\hbar\omega_0$ and $0.65\hbar\omega_0$, is a better fit for c-Si and c-Ge than the $f_1 = f_2 = 0.5$ fit, which assumes coupling to two phonons with energy $0.5\hbar\omega_0$.[9] They also showed that it is physically more reasonable because of its maximized joint density of states. In the high-T limit $A_1 \sim 1/f_1 + 1/f_2$, which explains why the A_{1i} obtained here assuming $f_1 = f_2 = 0.5$ are $\sim 10\%$ larger than the values obtained assuming $f_1 = 0.35$, $f_2 = 0.65$. Tang and Herman[13] showed that even near the respective melting points, the four-phonon term is not important in c-Si and c-Ge. This is also seen for the alloys; the inclusion of four-phonon coupling leads to negligibly small values of A_{2i} ($A_{2i}/A_{1i} < 0.01$).

The parameters for the model with $f_1 = 0.35, f_2 = 0.65, A_{2i} = 0$ are listed in Table II. In Fig. 3 these fits are plotted for the three modes for different x. These fits and the general trends vs x are not very sensitive to γ_i or ω_{0i}.

The parameters obtained for c-Si and c-Ge compare well with previously published results.[13] For c-Si, $A_1 = -3.4$ cm^{-1} here and -3.5 cm^{-1} in Ref. 13 (both with $\omega_0 = 528.0$ cm^{-1}). For c-Ge, $A_1 = -1.4$ cm^{-1} and $\omega_0 = 306.4$ cm^{-1}, whereas $A_1 = -1.2$ cm^{-1} and $\omega_0 = 306.2$ cm^{-1} in Ref. 13.

$|A_{1,\text{Si-Si}}|$ decreases with Ge fraction, much faster than does ω_0. $A_{1,\text{Ge-Si}}$ and $A_{1,\text{Ge-Ge}}$ depend on alloy concentration much more weakly. The change of $A_{1,\text{Ge-Ge}}$ as x increases from 0 to 0.15 and then to 0.29 is not monotonic, as is also seen for $d\omega/dT$ for this mode. Even though $d\omega/dT$, which also includes the effect of thermal expansion, is roughly the same for the three modes, $|A_{1,\text{Ge-Ge}}|$

is clearly $< |A_{1,\text{Si-Si}}|$. This is because $d\Delta_i^{(2)}/dT \sim A_{1i}/\omega_{0i}$ and $\omega_{\text{Ge-Ge}} \ll \omega_{\text{Si-Si}}$.

$|A_{1,\text{Si-Si}}|$ in Si-rich alloys is larger than $|A_{1,\text{Ge-Ge}}|$ in Ge-rich alloys, as is also true for $|A_1|$ normalized by the harmonic frequency, $|A_1|/\omega_0$. This is also seen when comparing optical phonons in c-Si and c-Ge. In contrast, in the Ge-rich alloy ($x = 0.29$), $|A_1|/\omega_0$ is smaller for the Si-Si mode than the Ge-Ge mode, and, in fact, it is largest for the Ge-Si mode. For the $x = 0.59$ alloy, $|A_1|/\omega_0$ is larger for the Ge-Si mode than for the Si-Si mode.

The Raman linewidth in c-Si and c-Ge is approximately equal to the phonon damping rate, which is the imaginary part of the phonon self-energy. In analogy with the Raman line shift, the linewidth of each of the alloy modes can be modeled as

$$\Gamma_{2i}(T) = B_{1i}\left\{1 + \sum_{j=1}^{2} \frac{1}{(e^{x_j}-1)}\right\}$$
$$+ B_{2i}\left\{1 + \sum_{k=1}^{3}\left[\frac{1}{(e^{y_k}-1)} + \frac{1}{(e^{y_k}-1)^2}\right]\right\}, \quad (5)$$

where x_j and y_k are defined as for Eq. (4). $\Gamma_{2i}(T)$ is similar to Eq. (4), with the first term corresponding to three-phonon processes (decay into two phonons), and the second term to four-phonon processes (decay into three phonons). It is assumed that there is an additional contribution to the linewidth of the alloy due to disorder that is independent of temperature, Γ_{1i}, as suggested by Herman and Magnotta.[16] The total linewidth $\Gamma_i(T)$ is then $\Gamma_{1i} + \Gamma_{2i}(T)$. Broadening due to phonon coupling is represented by a Lorentzian line shape. Though the disorder term is clearly not Lorentzian, since the overall profile is asymmetric, it is approximated as a Lorentzian here. Linewidth contributions due to compositional inhomogeneity are small and are ignored.

$\Gamma_2(T)$ is analyzed for the alloy assuming $f_1 = 0.35, f_2 = 0.65$ for the three-phonon term. Unlike the fit for $\Delta^{(2)}$, it is necessary to keep the four-phonon term. This has also been seen for c-Si and c-Ge by Tang and Herman.[13] For the Si-Si (Ge-Ge) modes, Γ_1 was set equal to $\Gamma_{\text{Si-Si(Ge-Ge)}} - \Gamma_{c\text{-Si}(c\text{-Ge})}$ at 295 K. For the Ge-Si mode at $x = 0.59$ Γ_1 was set equal to $\Gamma_{\text{Ge-Si}} - (\Gamma_{c\text{-Si}} + \Gamma_{c\text{-Ge}})/2$ at 295 K. A least-squares fit of $\Gamma(T)$ determined B_{1i} and B_{2i}, using ω_{0i} from the fit of $\omega(T)$. Furthermore, $\Gamma_2(T \to 0)$ was set equal to the low-temperature value of the "pure material," i.e., 1.30, 0.75, and 1.0 cm^{-1} for the Si-Si, Ge-Ge, and Ge-Si modes, respectively (from $\Gamma_{c\text{-Si}}(0)$, $\Gamma_{c\text{-Ge}}(0)$, and $[\Gamma_{c\text{-Si}}(0) + \Gamma_{c\text{-Ge}}(0)]/2$, respectively). The fit parameters are listed in Table III, and the fits are plotted with the data in Fig. 4.

The average instrumental linewidth of 2.8 cm^{-1} was used to analyze the GeSi and c-Si runs. For these materials, data analysis was insensitive to run-to-run variations about this average. However, for c-Ge it was necessary to use the 2.3-cm^{-1} instrumental linewidth measured during that run.

TABLE III. Parameters for fitting the Raman linewidth $\Gamma(T)$ for $Ge_{1-x}Si_x$ alloys with the $f_1=0.35, f_2=0.65$ model. Values of ω_0 from Table II are used in the fit of the data in Fig. 4. The uncertainty in B_1 is ± 0.05 cm^{-1} and B_2 is ± 0.01 cm^{-1}. Γ_{1i} is a temperature-independent contribution due to disorder. The c-Ge data were analyzed using a 2.3-cm^{-1} instrumental linewidth instead of the average value (2.8 cm^{-1}) used for the other runs.

Mode	x	$\Gamma_i(T=0)$ (cm^{-1})	Γ_{1i} (cm^{-1})	B_{1i} (cm^{-1})	B_{2i} (cm^{-1})
c-Si	1.0	1.3	0.0	1.28	0.04
Si-Si	0.92	3.3	2.0	1.28	0.07
	0.70	5.0	3.7	1.20	0.09
	0.59	9.2	7.9	1.21	0.06
Ge-Si	0.59	15.5	14.5	0.74	0.22
Ge-Ge	0.29	8.3	7.6	0.70	0.01
	0.15	6.4	5.8	0.56	0.06
c-Ge	0.0	0.6	0.0	0.54	0.06

The linewidth parameters agree reasonably well with those reported by Tang and Herman[13] for c-Si ($B_1=1.2254$ cm^{-1} and $B_2=0.0946$ cm^{-1}). For c-Ge, B_1 is smaller and B_2 is larger than that reported in Ref. 13 ($B_1=0.7352$ cm^{-1} and $B_2=0.0148$ cm^{-1}). These differences partially offset each other.

In the Si-rich alloy the dependence of the linewidth of the Si-Si mode on temperature is very similar to that of the optical phonon in c-Si, while in the Ge-rich alloy the Ge-Ge mode varies with T like the optical phonon in c-Ge. The Si-Si mode decays much faster than does the Ge-Ge mode. Note the large value of $B_{2,Ge-Si}$. This may mean that the four-phonon term is more important in the decay of the Ge-Si mode than for the Si-Si and Ge-Ge modes; however, uncertainties in the fit make any such conclusion highly uncertain. Table III suggests that $B_{1,Si-Si}$ may slightly decrease with increasing Ge fraction, while $B_{1,Ge-Ge}$ may increase with increasing Si fraction. However, because of scatter in the data in Fig. 4, and the uncertainties in the fitting procedure, it would be unwise to suggest such a trend. For the GeSi alloys in Refs. 18 and 19, Γ_{1i} would be expected to be smaller than the values listed in Table III, because those alloys have a narrower linewidth at 295 K.

IV. DISCUSSION

Overall, the temperature variation of the Raman shift and linewidth of the Si-Si mode in GeSi alloys is very similar to that for c-Si, while the variation of the Ge-Ge mode is similar to that for c-Ge. The dependence of the Ge-Si mode is intermediate. As the Ge fraction increases, there is a clear decrease in the coupling constant $|A_{1i}|$ that characterizes $\Delta^{(2)}(T)$ for the Si-Si mode. With the presented data, no such trends are discernible for B_{1i}.

The perturbation model used to fit the Raman spectra in Sec. III couples a Γ-point optical phonon to phonons that maximize the product of the anharmonic coupling constant and the joint density of final phonon states $g_2(\omega)$. If, in three-phonon coupling, the final states are two acoustic phonons (LA+TA) near the edges of the

Brillouin zone, as has been recently suggested by Narasimhan and Vanderbilt for c-Si,[14] then each of the three localized $Ge_{1-x}Si_x$ alloy optical vibrations couples to the more delocalized acoustic modes. The overall coupling in each case depends on the joint density of states for two acoustic phonons at the mode frequency $\omega_i(x)$. As noted for Si in Ref. 14, the coupling matrix element strongly depends on the wave vectors of the final-state phonons, so the details of $g_2(\omega)$ may not dominate $\Delta^{(2)}(T)$ [or $\Gamma_2(T)$].

Earlier, Menendez and Cardona[3] suggested that optical phonons in c-Si and c-Ge couple to an optical phonon (LO) and an acoustic phonon (LA) (both of which are off zone center, q$\neq$0). If such coupling occurs in the GeSi alloy, then it would be possible for, say, a $q \sim 0$ Si-Si optical phonon to couple to a $q \sim q'$ acoustic phonon and to either a Si-Si, Ge-Si, or Ge-Ge optical phonon with $q \sim -q'$. Though the spatial coupling between different optical modes, e.g., Si-Si with Ge-Si or Ge-Ge, could be weak, the joint density of states could be large. This mechanism would be fundamentally different from the anharmonic coupling mechanisms in c-Si and c-Ge. Perhaps the conservation of momentum restriction that forbids this coupling in c-Si (Ref. 14) is relaxed in these disordered GeSi alloys, and decay to LA-LO phonons can occur.

There is very little information about the joint density of states for phonons in GeSi alloys, even from higher-order Raman measurements. Since second-order Raman scattering is dominated by overtones, and not by the combination bands that are important here, it reflects the single-phonon density of states $g_1(\omega)$ scaled in ω by two. Some information can be gleaned from c-Si and c-Ge and from measurements of $g_1(\omega)$ for the alloy. The c-Si and c-Ge phonon-dispersion relations very nearly scale, except for the zone-boundary TA phonons, and therefore $g_1(\omega)$ and $g_2(\omega)$ for Si and Ge are nearly homologous.[34,35] For both, $g_1(\omega)$ has a peak near $0.65\omega_0$ due to LA(L) phonons and a peak at $0.35\omega_0$ due to acoustic phonons along Σ, but $g_1(0.5\omega_0)$ is negligible. This justifies the use of the $f_1=0.35, f_2=0.65$ model for c-Si and c-Ge, as suggested in Refs. 3 and 14, and the rejection of the $f_1=f_2=0.5$ model, earlier suggested in Refs. 4 and 9. This is probably also true for the Si-Si mode for $x \sim 1$ alloys and the Ge-Ge mode for $x \sim 0$ alloys, for which the anharmonic coupling constants and $g_2(\omega)$ are probably very similar to those for c-Si and c-Ge, respectively. This is much less certain for other x and for the Ge-Si mode.

Because of the lack of inelastic neutron-scattering data, $g_1(\omega)$ for c-GeSi must be deduced from first-order Raman scattering from a-GeSi and second-order Raman scattering from c-GeSi.[20,36-39] The reduced Raman intensity of a-Si (a-Ge) has been shown to be a good measure of $g_1(\omega)$ for c-Si (c-Ge), broadened somewhat and shifted (by ~ -10 cm^{-1}).[36] The Raman spectrum of a-GeSi (Refs. 37 and 39) is continuous, with relatively sharp features near $x=0$ and 1, and broad features near $x=0.5$. The TA peak moves from ~ 90 cm^{-1} for a-Ge to ~ 180 cm^{-1} for a-Si. It also has prominent features at

~ 280, ~ 390, and ~ 480 cm^{-1} due to Ge-Ge, Ge-Si, and Si-Si optical vibrations, respectively. The position of these features vary little with x, though their amplitudes vary according to the number of Ge-Ge, Ge-Si, and Si-Si pairs. Similar, but sharper features are seen in second-order Raman-scattering[38] and tunneling measurements.[40] $g_1(\omega)$ inferred from these measurements are in accord with the models of Dean[41] and Yndurain.[42]

Overall, $g_1(\omega)$ is expected to be appreciable at $0.35\omega_{0i}$ and $0.65\omega_{0i}$ for each of the three alloy modes at all compositions investigated here; however, nothing specific can be inferred about $g_2(\omega)$. Still, the $f_1 = 0.35, f_2 = 0.65$ model is expected to be reasonable for phonon coupling in GeSi alloys, at least for the Si-Si mode near $x = 1$ and the Ge-Ge mode near $x = 0$. Because $\omega_{Ge-Ge} \sim 0.6\omega_{Si-Si}$ and $\omega_{Ge-Si} \sim 0.8\omega_{Si-Si}$, it is possible that the Si-Si mode couples through either of these two optic modes. Then f_1 and f_2 would also be different than for c-Si or c-Ge. However, since $|A_{1,Si-Si}|$ tends to decrease with x, this potential new pathway does seem to be very significant. Overall, it is not clear how the anharmonic coupling term and joint density of states vary with x for the three modes.

The dependence of the joint density of states on alloy composition can affect A_{1i} in another way. The three-phonon term in $\Delta^{(2)}$ is the product of A_{1i} and a term linearly dependent on the phonon density $[\sim(1/f_1 + 1/f_2)/\omega_{0i}$ at high $T]$. A_{1i} can be approximated as the product of the anharmonic coupling constant and the joint density of states for final-state phonon energies (f_1, f_2) for which this product is maximum. If, for a given mode, f_1 and f_2 change with x, and this change is not reflected in the calculation, the value obtained for A_{1i} would be wrong. For example, if the Si-Si mode decayed into phonons of equal energy $(f_1 = f_2 = 0.5)$ for $x = 0.29$ or 0.59, rather than $0.35\hbar\omega_0$ and $0.65\hbar\omega_0$ for $x \sim 1$, $|A_{1i}|$ would be 10% higher than that presented in Table II. Since this is the maximum increase possible by this consideration, it cannot account for the entire change of $A_{1,Si-Si}$ with x.

By comparing first- and second-order Raman spectra in polycrystalline GeSi, Lannin[20] showed that Raman scattering involves only near-zone-center $\mathbf{q} \sim 0$ phonons through much of the composition range; however, he showed that disorder can lead to the nonconservation of momentum at extreme alloy concentrations, as for the Ge-Ge mode when $x \sim 1$. Earlier work by Renucci, Renucci, and Cardona[25] suggested that zone-edge phonons may dominate scattering even for $x \sim 0.5$. It is possible that the observed decrease in $|A_{1,Si-Si}|$ for large Ge fractions may be due, in part, to this effect of disorder.

The potential importance of such disorder can be revealed by studies of $\omega(T)$ for optical phonons away from the zone center in Si and Ge. These phonons become more important in Raman scattering as disorder increases. By studying two-phonon scattering, Tsu and Hernandez[5] showed that in c-Si $(d\omega/dT)/\omega$ is the same $(-5.4 \times 10^{-5}/K)$ for $\mathbf{q}=0$ LO/TO phonons $(\Gamma_{25'})$, and TO phonons at L $(L_{3'})$, and that it is smaller for TO phonons at X (X_4) $(-3.6 \times 10^{-5}/K)$. They also provide

data that suggest that $(d\omega/dT)/\omega$ is $\sim 0-10\%$ smaller for a-Si than for $\Gamma_{25'}$ phonons in c-Si. In c-Ge, Nelin and Nilsson[43] showed that $(d\omega/dT)/\omega$ is the same within $\sim 10\%$ for $\Gamma_{25'}$, X_1 (LO at X), $L_{3'}$, and L_1 (LO at L) optical phonons $(-5.1 \times 10^{-5}/K)$, but that it is larger in magnitude by $\sim 40\%$ at X_4. Therefore, to first order $(d\omega/dT)/\omega$ is fairly constant across the Brillouin zone in c-Si and c-Ge.

$d\omega/dT$ is affected by volume expansion and phonon coupling. Given the generally larger γ for optical phonons away from the zone center $(\sim 1.1-1.5)$ than at $\mathbf{q}=0$ in Si and Ge (~ 1.0),[44,45] the fraction of $d\omega/dT$ due to volume expansion is generally larger for $\mathbf{q} \neq 0$ phonons, and, therefore, the fraction due to phonon coupling is relatively smaller.

Comparison of a-Si with c-Si shows the effect of complete long-range disorder. If $(d\omega/dT)/\omega$ and γ were the same for a-Si and c-Si at $\Gamma_{25'}$, then $|A_1|$ would still be smaller by $\sim 15\%$ for a-Si relative to c-Si. This is due to the relative factor of $(\omega_{a-Si}/\omega_{c-Si})^2$ that comes from $(d\omega/dT)/\omega$, and the high-T expansion of $\Delta^{(2)}(\omega_{a-Si} \sim 480$ cm^{-1}, and $\omega_{c-Si} = 521$ cm$^{-1})$. Using more realistic values for γ_{a-Si} of 1.3 (from an average over the c-Si Brillouin zone) or 2.0 (which comes from data in Ref. 46, and which seems too high), $|A_1|$ would be smaller by 20% or 33% in a-Si than in c-Si, assuming equal $(d\omega/dT)/\omega$, or by 31% or 43% if $|(d\omega/dT)/\omega|$ is smaller in a-Si by 10%. Therefore, disorder could account for part of the $\sim 47\%$ decrease in $|A_{1,Si-Si}|$ as x decreases from 1 to 0.29.

The observed nonmonotonic change in $|A_{1,Ge-Ge}|$, an increase from $x = 0$ to 0.15 followed by a decrease with increasing x, cannot be attributed to uncertainties in α, γ, or the current measurements. It is noted that other properties of $Ge_{1-x}Si_x$ alloys change abruptly near $x = 0.15$, such as the coefficient of thermal expansion,[33] which is also related to anharmonicity, and the variation of the band gap with x, which is due to the change from Ge to Si-like conducting-band minima.[1]

The anharmonic shift at $T = 0$ is $A_{1i} + A_{2i}$, which is $\sim A_{1i}$ here. Vanderbilt, Louie, and Cohen[47] have shown that for Si and Ge this shift can be approximated by $[3\hbar/4M^2\omega_0^2](\tilde{\alpha}+2\tilde{\beta}) - [3\hbar/4M^3\omega_0^4]\tilde{\gamma}^2$, where the first term is due to quartic interactions in first-order perturbation theory, described by anharmonic coupling constants $\tilde{\alpha}$ and $\tilde{\beta}$, and the second term is due to cubic terms in second order, as described by $\tilde{\gamma}$. M is the atomic mass. Both terms $\sim T$ at high T, though only the second term has the explicit form of the first term in Eq. (4). The calculation in Ref. 47 predicts $A_1 = -3.5$ and -1.2 cm^{-1} for c-Si and c-Ge, respectively, which is close to the observed values, with $\sim 80\%$ of A_1 due to the cubic term. One way to compare A_{1i} for the different alloy modes is to assume that there are such alloy-averaged parameters $\tilde{\alpha}$, $\tilde{\beta}$, and $\tilde{\gamma}$, and then to compare either $M_i^2\omega_{0i}^2 A_{1i}$ or $M_i^3\omega_{0i}^4 A_{1i}$, which are A_{1i} scaled to give the quartic term $\tilde{\alpha}+2\tilde{\beta}$ and the cubic term $\tilde{\gamma}^2$, respectively, within a constant. M_i is the Si (Ge) mass for the Si-Si (Ge-Ge) mode, and it is twice the Si/Ge reduced mass for the Ge-Si mode. Figure 5 shows quartic scaling of A_{1i}. Both ways
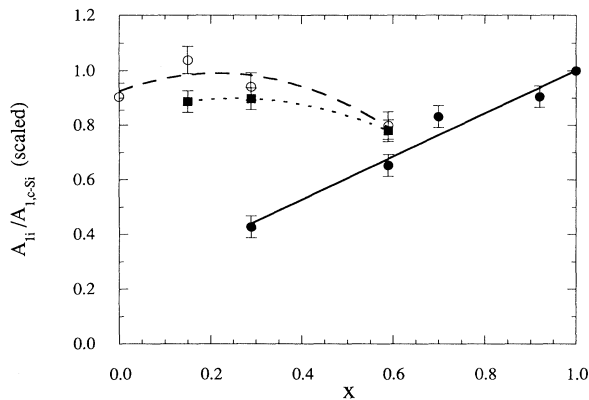
FIG. 5. Scaled values of A_{1i} for the three modes, normalized to the value in c-Si. The scaling relationship for the quartic anharmonic parameters, $M_i^2\omega_{0i}^2 A_{1i}$, is used. The solid circles, solid squares, and open circles represent the Si-Si, Ge-Si, and the Ge-Ge modes, respectively. The curves through the points, which are solid, dotted, and dashed, respectively, are meant to aid viewing.

of scaling A_{1i} give qualitatively the same results, with fairly uniform anharmonic parameters for the three modes for all x, except for the Si-Si mode in the Ge-rich alloy, where the scaled $|A_{1i}|$ becomes very small.

The variation of linewidth with temperature also depends on the product of anharmonic coupling constants and $g_2(\omega)$. On the basis of the frequency shift data, it is not surprising that B_{1i} for the Si-Si (Ge-Ge) modes for $x \sim 1(0)$ is approximately that for optical phonons in c-Si (c-Ge). Narasimhan and Vanderbilt[14] have calculated $\Gamma(T)$ for c-Si at various points in the Brillouin zone. Their calculation included only the cubic anharmonic terms that contribute to three-phonon coupling (B_1), which explains why they predict smaller linewidths for zone-center phonons than are measured. Still, they found

that $d\Gamma/dT$ is significantly smaller (larger) for LO(TO) modes at the X and L points than at the zone center. Since probably both LO and TO modes contribute in the backscattering from polycrystalline GeSi alloys, these calculations have no clear implications for these experiments.

V. CONCLUDING REMARKS

The temperature dependence of the Raman shift of the three GeSi alloy modes is well described by considering the volume expansion and three-phonon coupling anharmonic contributions to the real part of the phonon self-energy. Four-phonon coupling is not important. The Raman shift of the Si-Si (Ge-Ge) mode in the alloy has a temperature dependence very much like that of the c-Si (c-Ge) optical mode for Si-rich (Ge-rich) alloys. The Si-Si mode frequency changes much more slowly with temperature in Ge-rich than in Si-rich alloys. This is due to changes in the coupling matrix elements and final-state joint density of states with x, and is possibly also affected by mechanisms that may occur in GeSi alloys but not in c-Si and c-Ge. These mechanisms depend on the possible additional coupling to other optical phonon modes and on the possible non-zone-center nature of the optical phonon formed in Stokes scattering. Though the shift of the Ge-Si mode depends on temperature in a way similar to Si-Si and Ge-Ge modes, it is difficult to make a quantitative comparison. The variation of the Raman peak width in the alloy with temperature is modeled by three- and four-phonon decay processes, as in c-Si and c-Ge, and a temperature-independent disorder term.

[1]J. C. Bean, Science **230**, 127 (1985).

[2]H. Bottger, *Principles of the Theory of Lattice Dynamics* (Physik Verlag, Berlin, 1983).

[3]J. Menendez and M. Cardona, Phys. Rev. B **29**, 2051 (1984).

[4]M. Balkanski, R. F. Wallis, and E. Haro, Phys. Rev. B **28**, 1928 (1983).

[5]R. Tsu and J. G. Hernandez, Appl. Phys. Lett. **41**, 1016 (1982).

[6]T. R. Hart, R. L. Aggarwall, and B. Lax, Phys. Rev. B **1**, 638 (1970).

[7]R. K. Ray, R. L. Aggarwall, and B. Lax, in *Light Scattering in Solids,* edited by M. Balkanski (Flammarion, Paris, 1971), p. 288.

[8]R. A. Cowley, J. Phys. (Paris) **26**, 659 (1965).

[9]P. G. Klemens, Phys. Rev. **148**, 845 (1966).

[10]E. Haro, M. Balkanski, R. F. Wallis, and K. H. Wanser, Phys. Rev. B **34**, 5358 (1986).

[11]C. Z. Wang, C. T. Chan, and K. M. Ho, Phys. Rev. B **40**, 3390 (1989).

[12]R. J. Nemanich, D. K. Biegelsen, R. A. Street, and L. E. Fennell, Phys. Rev. B **29**, 6005 (1984).

[13]H. Tang and I. P. Herman, Phys. Rev. B **43**, 2299 (1991).

[14]S. Narasimhan and D. Vanderbilt, Phys. Rev. B **43**, 4541 (1991).

[15]G. D. Pazionis, H. Tang, and I. P. Herman, IEEE J. Quantum

Electron. **25**, 976 (1989).

[16]I. P. Herman and F. Magnotta, J. Appl. Phys. **61**, 5118 (1987).

[17]M. I. Alonso and K. Winer, Phys. Rev. B **39**, 10 056 (1989).

[18]M. A. Renucci, J. B. Renucci, and M. Cardona, in *Light Scattering in Solids* (Ref. 7), p. 326.

[19]W. J. Brya, Solid State Commun. **12**, 253 (1973).

[20]J. S. Lannin, Phys. Rev. B **16**, 1510 (1977).

[21]H. D. Fuchs, C. H. Grein, M. I. Alonso, and M. Cardona, Phys. Rev. B **44**, 13 120 (1991).

[22]G. M. Zinger, I. P. Ipatova, and A. V. Subashier, Fiz. Tekh. Poluprovodn. **11**, 656 (1977) [Sov. Phys. Semicond. **11**, 383 (1977)].

[23]B. A. Weinstein and G. J. Piermarini, Phys. Rev. B **12**, 1172 (1975).

[24]D. Olego and M. Cardona, Phys. Rev. B **25**, 1151 (1982).

[25]J. B. Renucci, M. A. Renucci, and M. Cardona, Solid State Commun. **9**, 1651 (1971).

[26]T. Ishidate, S. Katagiri, K. Inoue, M. Shibuya, K. Tsuji, and S. Minomura, J. Phys. Soc. Jpn. **53**, 2584 (1984).

[27]Z. Sui, H. H. Burke, and I. P. Herman, Phys. Rev. B **48**, 2162 (1993).

[28]J. C. Brice, *Crystal Growth Processes* (Wiley, New York, 1986).

[29]J. P. Dismukes and L. Ekstrom, Trans. Met. Soc. AIME **233**, 672 (1965).

[30]H. H. Burke, V. Tavitian, J. G. Eden, and I. P. Herman, Appl. Phys. Lett. **55**, 253 (1989).

[31]V. A. Gaisler, I. G. Neizvestnyi, M. P. Sinyukow, and A. B. Talochkin, Fiz. Tverd. Tela (Leningrad) **30**, 806 (1988) [Sov. Phys. Solid State **30**, 462 (1989)].

[32]C. Postmus, J. R. Ferraro, and S. S. Mitra, Phys. Rev. **174**, 983 (1968).

[33]*Numerical Data and Functional Relations in Science and Technology*, edited by O. Madelung, M. Schultz, and H. Weiss, Landolt-Börnstein, New Series, Group III, Vol. 17, Part a (Springer-Verlag, Berlin, 1982), and references therein.

[34]G. Dolling and R. A. Cowley, Proc. Phys. Soc. London **88**, 463 (1966).

[35]G. Nilsson and G. Nelin, Phys. Rev. B **6**, 3777 (1972).

[36]J. E. Smith, Jr., M. H. Brodsky, B. L. Crowder, and M. I. Nathan, in *Light Scattering in Solids* (Ref. 7), p. 330.

[37]J. S. Lannin, in *Proceedings of the Fifth International Conference on the Physics of Amorphous and Liquid Semiconductors*, edited by J. Stuke and W. Brenig (Taylor & Francis, London, 1974), p. 1245.

[38]J. S. Lannin, Solid State Commun. **19**, 35 (1976).

[39]N. J. Shevchik, J. S. Lannin, and J. Tejeda, Phys. Rev. B **7**, 3987 (1973).

[40]R. A. Logan, J. M. Rowell, and F. A. Trumbone, Phys. Rev. A **136**, 1751 (1964).

[41]P. Dean, Rev. Mod. Phys. **44**, 127 (1972).

[42]F. Yndurain, Phys. Rev. B **18**, 2876 (1977).

[43]G. Nelin and G. Nilsson, Phys. Rev. B **10**, 612 (1974).

[44]C. H. Xu, C. Z. Wang, C. T. Chan, and K. M. Ho, Phys. Rev. B **43**, 5024 (1991).

[45]S. de Gironcoli, Phys. Rev. B **46**, 2412 (1992).

[46]T. Ishidate, K. Inoue, K. Tsuji, and J. Minomura, Solid State Commun. **42**, 197 (1982).

[47]D. Vanderbilt, S. G. Louie, and M. L. Cohen, Phys. Rev. B **33**, 8740 (1986).